POLITECNICO DI TORINO
Repository ISTITUZIONALE

Performance Comparison of Translucent C-band and Transparent C+L-band Network

Original
Performance Comparison of Translucent C-band and Transparent C+L-band Network / Sadeghi, R., DE ARAUJO CORREIA, B.V., Virgillito, E., Napoli, A., Costa, N., Pedro, J., Curri, V.. - ELETTRONICO. - (2021), pp. 1-3. (2021 Optical Fiber Communications Conference and Exhibition, OFC 2021 Washington, DC United States 6–11 June 2021).

Availability:
This version is available at: 11583/2927951 since: 2021-09-29T10:18:28Z

Publisher:
OSA

Published
DOI:

Terms of use:

This article is made available under terms and conditions as specified in the corresponding bibliographic description in the repository

Publisher copyright
Optica Publishing Group (formely OSA) postprint/Author's Accepted Manuscript

"© 2021 Optica Publishing Group. One print or electronic copy may be made for personal use only. Systematic reproduction and distribution, duplication of any material in this paper for a fee or for commercial purposes, or modifications of the content of this paper are prohibited."

(Article begins on next page)

03 November 2026

Performance Comparison of Translucent C-band and Transparent C+L-band Network

Rasoul Sadeghi[1], Bruno Correia[1], Emanuele Virgillito[1], Antonio Napoli[2], Nelson Costa[3], João Pedro[3,4], and Vittorio Curri[1]

[1] *DET, Politecnico di Torino, C.so Duca degli Abruzzi 24, 10129 Torino, Italy;* [2] *Infinera, UK;* [3] *Infinera Unipessoal Lda, Rua da Garagem 1, 2790-078 Carnaxide, Portugal;* [4] *Instituto de Telecomunicações, Instituto Superior Técnico, Avenida Rovisco Pais 1, 1049-001 Lisboa, Portugal*

rasoul.sadeghi@polito.it

Abstract: We compare transparent and translucent network design in terms of capacity, energy consumption, and cost. Results show that exploiting extra spectrum bands is more beneficial than deploying additional regenerators in the C-band. © 2020 The Author(s)

OCIS codes: 060.0060, 060.4256.

1. Introduction

To cope with the continuous increase of network traffic boosted, for example, by the worldwide COVID-19 pandemic [1], it is urgent to increase the capacity of wavelength-division multiplexing (WDM) systems – that nowadays operate in C-band only with a spectrum of around 4.8 THz. Elastic optical networks (EON) are an important step to fully exploit the C-band by allowing to adapt the amount of spectrum allocated according to the specifics of each lightpath (LP). Another key strategy is to enforce traffic grooming to maximize the utilization of the already deployed transceivers (TRXs) [2]. Simultaneously, minimizing the overall power consumption is an economic imperative for network operators, as well as a societal objective, further motivating the use of high capacity as well as power-efficient TRXs [3]. The energy consumption of different TRXs has been investigated in [4], where it is highlighted that Intel's integrated circuit CMOS node size decreases every two years. The Optical Internetworking Forum (OIF) provides an implementation agreement (IA) for pluggable form factors based on coherent-detection [5]. The latest IA is the 400ZR [1], which defines a power-efficient and cost-effective coherent interface that supports 400 Gbps with a symbol rate of 59.84 Gbaud [6]. Despite the reported progress in the coherent interfaces, the continuous traffic growth will lead to capacity exhaustion. Rolling-out or leasing additional fibers is a solution to cope with this issue, but it is often the last resort, particularly in long-haul and regional networks. Alternatively, operators have two main options to increase capacity in the short-term: (i) upgrade their line systems to support C+L-band; (ii) make use of regenerators to increase the capacity and spectral efficiency of the deployed LPs. In [7], optical power adaptation in translucent optical networks has been investigated by extending the generalized multiprotocol label switching (GMPLS) to support optical regeneration. In this work, we compare the capacity, energy consumption, and cost of two different coherent TRXs, designated as Flex and Fix rate. A traditional transparent network design is used with Flex rate TRX, via adapting the modulation format to the physical path characteristics. A translucent network design is used with Fix rate TRXs, which resorts to intermediate regenerators for error-free end-to-end transmission. A statistical network assessment [8] over the German network topology with uniform [9] traffic distribution is reported with extensions developed to cover all the described scenarios, such as adding different TRXs based on commercial specifications and implementing a regenerator placement algorithm based on the QoT of the LPs. For benchmarking purposes, we also investigate the network performance when employing ideal Shannon TRXs. The transparent network design (Flex) is considered for both C- and C+L-band scenarios, whereas translucent network design (Fix) is evaluated for the C-band only.

2. QoT abstraction and regenerator placement

When coherent TRXs only are considered, the performance of a LP can be modeled based on two Gaussian disturbances: ASE noise and nonlinear interference (NLI), introduced by the amplifiers and fiber propagation, respectively. In this scenario, the quality of transmission (QoT) at the end of each fiber span can be estimated by the generalized signal-to-noise ratio (GSNR) [9]. The NLI evaluation can resort to the generalized Gaussian noise (GGN) model, including both spectral and spatial variation of gain/loss and its interaction with the stimulated Raman scattering (SRS) effect [10]. Following a disaggregated approach [11], the QoT of the LP can be determined by: $\mathrm{GSNR}_{i,\mathrm{total}} = 1/\sum_{s\in L}(\mathrm{GSNR}_{i,s})^{-1}$, where $\mathrm{GSNR}_{i,s}$ denotes the GSNR of i_{th} frequency on span s of the LP. In Fig. 1(b) we present the GSNR profile for a 75 km span of a standard single mode fiber (SSMF), in both scenarios modeled in this work: C-band only and C+L-band. C-Band only delivers an average GSNR of 30.55 dB with a 0.79 dB difference between the maximum and minimum values. However, enabling L band in BDM case GSNR values changes to 29.76 dB and 30.64 dB of average GSNR with 1.08 dB and 0.97 dB difference between the maximum and minimum values on C and L band, respectively. Therefore,

[1] 400ZR IA defines only 400G transmission with 16QAM $<$ 120km. Nevertheless, it is a common assumption in the industry that the technology will be leveraged in pluggable interfaces also supporting lower order modulation formats. This is often designated as OpenZR+.

about 1 dB of QoT degradation going from C to C+L band accounts for the further NLI and SRS effect added by lighting up the L-band. A total of 64 and 128 channels on the ITU-T 75 GHz grid with Rs=64 Gbaud have been considered for C-band and C+L-band, respectively. The German network topology is considered which contains 17 nodes, 26 edges, and the average distance between two ROADM nodes is 207 km for an overall covered area with a diameter of 600 km and an average node degree of 3.1. The k-shortest path algorithm is utilized to compute up to $k_{max} = 15$ candidate routing paths and a best-SNR wavelength assignment policy is enforced. A progressive traffic load analysis is performed, where each new request demands 100 Gbps of traffic. The possibility of doing traffic grooming is evaluated before the establishment of a new LP by verifying if any of the already deployed LPs has enough capacity to accommodate the new request (end-to-end). Flex TRXs are deployed using a transparent network design approach for both C- and C+L-band cases.

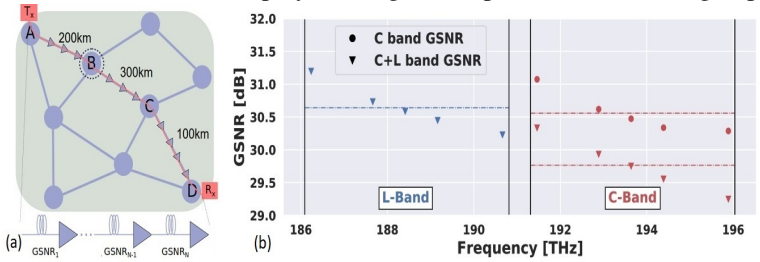


Fig. 1: (a) Regenerator placement example and (b) GSNR profiles for a single 75 km span in C and C+L band transmission.

Table 1: TRXs modelling assumptions.

TRX	mod. form.	Data rate [Gb/s]	Typical reach [km]	P[W]
Flex	16QAM	400	L<120	15
	16QAM	400	120<L<450	20
	8QAM	300	450<L<1500	18
	QPSK	200	1500<L<2500	16
	QPSK	100	2500<L	13
Fix	16QAM	400	L<120	15
	16QAM	400	120<L<450	20

According to Table 1, Flex TRX type supports multiple modulation formats with different maximum reach figures. When a new request arrives, the SNAP control plane selects the proper modulation format based on the estimated QoT and length between the source and destination. For instance, in Fig. 1(a) the length of request (source: node A, destination: node D) is 600 km. So, a transparent network with Flex TRX would use, for example, 8QAM (300Gbps) or even a less efficient modulation format (<300Gbps), depending on the estimated QoT of the path. Unlike the transparent case, the translucent network design assumes the use of Fix TRX, which supports only the 16QAM modulation format. In this configuration, the TRX consumes 15 W in short distances (< 120km) and 20 W for long distances (120km<L<450km), as mentioned in Table 1. In the translucent case, regenerators (realized as a pair of back-to-back TRXs) can be used at intermediate nodes to achieve the required QoT to set up the end-to-end connection. Regenerator assignment in this type of network is based on both the QoT and the maximum reach that the TRX supports. Although potentially requiring more TRXs, this design strategy has the advantage of maximizing the spectral efficiency and relaxing the impact of the spectrum continuity constraint, thereby allowing to increase the traffic load. In Fig. 1(a), it is observable that when the same request arrives (A-D), the SNAP control plane continuously checks the QoT and length of LPs. Note that the latter is used to verify if the accumulated chromatic dispersion is within the TRX operating limits. If QoT is higher than the required GSNR [13] for 16-QAM and the total length is smaller than the maximum reach supported by the TRX, the algorithm does not assign a regenerator. Otherwise, one or more regenerators are required at intermediate nodes. In the example of Fig. 1(a), a regenerator needs to be placed in the intermediate node B because at this node the two LPs [(A-B), (B-D)] meet the requirements of minimum QoT and maximum reach. Noteworthy, the SNAP control plane avoids deploying unnecessary regenerators, consequently preventing further increases in cost. Comparing both scenarios (Transparent using C+L transmission and translucent using C-band only), it is possible to evaluate the pros and cons of each strategy, with the former one increasing the overall network capacity without increasing the average energy consumption and costs in the network.

3. Network simulation results and discussion

The capacity and energy consumption when deploying transparent and translucent networks is analyzed in this section. Fig. 2 depicts the impact of increasing the traffic load on the blocking probability (BP) and energy consumption when considering different network designs. The capacity obtained with ideal TRXs (which assume the Shannon limit) is shown to highlight the theoretical maximum capacity on the C-band. Fig. 2(a) shows that the transparent network with Flex TRXs results in higher BP than the translucent network with Fix TRXs, when considering the C-band only. A closer observation, as summarized in Table 2, highlights that the capacity of the translucent network is 25% higher than that of the transparent network with C-band only at BP=10^{-2}. This is a consequence of deploying LPs only with the most spectral efficient format available and of reducing the impact of the spectrum continuity constraint. However, its energy consumption per bit, which is shown in Fig. 2(b), is almost 4 dB higher than the transparent network at the same BP (marked with θ). To increase network capacity, L-band with a total bandwidth of 4.8 THz, leading to a C+L band system with a total bandwidth of 9.6 THz, is also enabled (in the transparent network design). This results in a significant increase of capacity, which more than doubles, compared to the transparent case with C-band only. The higher availability of channels eases the spectrum continuity constraint and explains the reason for an increase that exceeds a factor of two. On the other

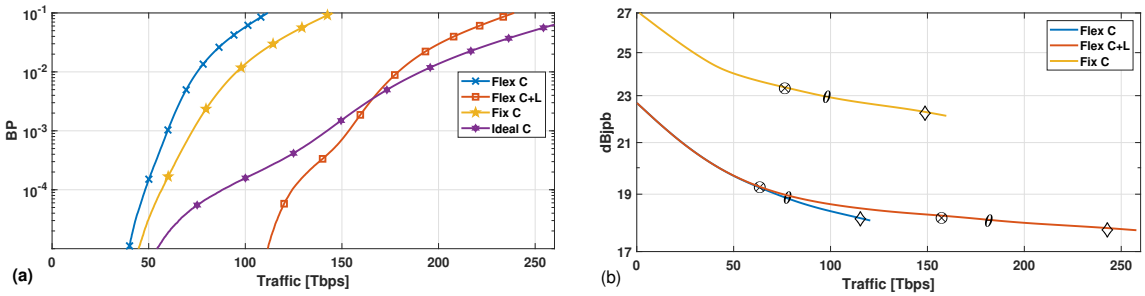


Fig. 2: (a) Allocated traffic versus blocking probability (BP) and (b) allocated traffic versus dB joule per bit. The energy consumption at BP 0.1%, 1%, and 10% are marked with $\otimes$, θ, and $\diamondsuit$, respectively.

hand, the energy consumption per bit remains almost the same as when considering C-band only, even showing a slight decrease at BP of 1%. It should be noticed that the introduction of L-band demands C+L-band amplifiers which will have a higher power consumption than C-band only amplifiers. Nevertheless, the power consumption of the network is usually dominated by the TRXs and not by the amplifiers. Another relevant observation is that at low loads the BP with C-band only configurations is significantly higher than that with C+L-band. This is a consequence of having twice the number of channels in the latter case, enabling to set up LPs between a higher number of node pairs. As traffic load increases the trends associated with the different TRXs and design options become more clear. For instance, with Ideal TRX, the fact that very high capacity (i.e., > 400Gbps) and spectral efficient LPs are set up at low loads, enables to accommodate the incoming traffic requests without setting up many new LPs. This explains the smoother evolution of the BP curve and, as shown in Table 2, this configuration enables to carry up to 2.5 times the traffic load of the Flex C-band case for a BP=10^{-2}. Fig.3 gives further insight on the power consumption figures by showing the average number of new LPs (and TRX pairs) being created as traffic increases. At small loads, there is the need to create new LPs since node pairs have no LP between them. Afterward, only a few new LPs need to be set up, since grooming over the existing LPs enables to efficiently utilize the existing ones. It is clear from this plot that the Fix C-band case is the one that results in the creation of more LPs, and the consequent provisioning of more TRXs, as a result of using intermediate regenerators. Flex C-band and C+L-band have a similar trend in terms of the average number of LP while BP is approximately the same. Table 2 also summarizes the number of TRXs, normalized to the number of end-to-end connections that are set up, highlighting that Fix C-band results in a very costly design, while only providing a capacity improvement of up to 25%. On the other hand, Flex C+L-band more than doubles the amount of usable capacity without increasing significantly the number of normalized TRXs required nor the power consumption.

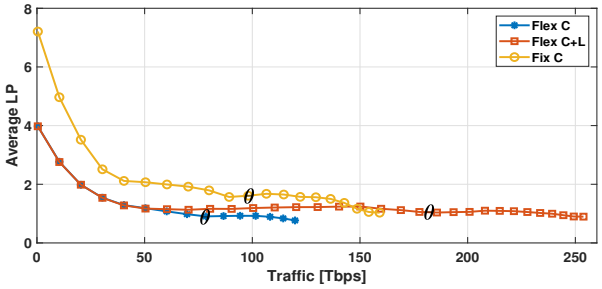


Fig. 3: Average allocated LP versus traffic.

Table 2: Multiplicative factor at BP = 1% (with respect to Flex C).

	Total Traffic	Total Energy	Normalized TRX Count
Flex C	1	1	1
Flex C+L	2.36	0.95	1.06
Fix C	1.25	1.21	1.72
Ideal C	2.52	-	0.07

4. Conclusions

In this work, we showed that the utilization of regenerators to enable higher order modulation formats has a limited impact in increasing capacity, while augmenting cost and power consumption. Exploiting the C+L-band and flexible transceivers is shown to be more effective. Alternatively, using state-of-the-art transceivers (i.e., performing closer to the Shannon limit) could also allow to significantly increase capacity using only the C-band.

Acknowledgment

This work was partially funded by the EU H2020 within the ETN WON, grant agreement 814276 and by the Telecom Infra Project.

References

1. OECD, "Keeping the internet up and running intimes of crisis," tech. rep.
2. G. Zhang, et al., JOCN., vol. 4, pp. B17–B25, Nov 2012.
3. F. Musumeci, et al., JOCN, vol. 4, pp. 108–117, Feb 2012.
4. W. M. Holt, ISSCC, pp. 8–13, 2016.
5. F. Frey et al., Photonic Networks; 18. ITG-Symposium, pp. 1–8, 2017.
6. "OIF 400ZR IA." *https://www.oiforum.com/wp-content/uploads/OIF-400ZR-01.0,reduced2.pdf*
7. M. Kanj et al., JOCN, vol. 10, no. 9, pp. 760–772, 2018.
8. V. Curri et al., JLT, vol. 35, no. 6, pp. 1211–1221, 2017.
9. E. Virgillito et al., OFC, p. M2G.4,2020.
10. M. Cantono et al., JLT, vol. 36,no. 15, pp. 3131–3141, 2018.
11. V. Curri, ICTON, 2020, p. We.C2.1, IEEE, 2018
12. E. Virgillito et al., ONDM, pp. 1–6, 2020.
13. J. Pedro et al., ICTON, pp. 1–6, 2018.
14. M. Cantono et al., JLT, vol. 38,no. 5, pp. 1050-1060, 2020.